Institut Pasteur

Microbes and Infection 14 (2012) 59–68

www.elsevier.com/locate/micinf

Original article

Early dystrophin disruption in the pathogenesis of experimental chronic Chagas cardiomyopathy

Cibele M. Prado [a,d], Mara R.N. Celes [a], Lygia M. Malvestio [a], Erica C. Campos [a], João S. Silva [b], Linda A. Jelicks [c], Herbert B. Tanowitz [d], Marcos A. Rossi [a,*]

[a] *Department of Pathology, Faculty of Medicine of Ribeirão Preto, University of São Paulo, S.P., Brazil*
[b] *Department of Biochemistry and Immunology, Faculty of Medicine of Ribeirão Preto, University of São Paulo, S.P., Brazil*
[c] *Department of Physiology and Biophysics, Albert Einstein College of Medicine, Bronx, NY, USA*
[d] *Department of Pathology, Albert Einstein College of Medicine, Bronx, NY, USA*

Received 28 April 2011; accepted 17 August 2011
Available online 31 August 2011

Abstract

Chronic Chagas cardiomyopathy evolves over a long period of time after initial infection by *Trypanosoma cruzi*. Similarly, a cardiomyopathy appears later in life in muscular dystrophies. This study tested the hypothesis that dystrophin levels are decreased in the early stage of *T. cruzi*-infected mice that precedes the later development of a cardiomyopathy. CD1 mice were infected with *T. cruzi* (Brazil strain), killed at 30 and 100 days post infection (dpi), and the intensity of inflammation, percentage of interstitial fibrosis, and dystrophin levels evaluated. Echocardiography and magnetic resonance imaging data were evaluated from 15 to 100 dpi. At 30 dpi an intense acute myocarditis with ruptured or intact intracellular parasite nests was observed. At 100 dpi a mild chronic fibrosing myocarditis was detected without parasites in the myocardium. Dystrophin was focally reduced or completely lost in cardiomyocytes at 30 dpi, with the reduction maintained up to 100 dpi. Concurrently, ejection fraction was reduced and the right ventricle was dilated. These findings support the hypothesis that the initial parasitic infection-induced myocardial dystrophin reduction/loss, maintained over time, might be essential to the late development of a cardiomyopathy in mice.

Keywords: Chronic Chagas cardiomyopathy; Dystrophin; Chagas disease; Dystrophinopathy; *Trypanosoma cruzi*

1. Introduction

One of the most intriguing aspects of chronic Chagas cardiomyopathy (CCC) is that it evolves over a long period of time after initial infection by the protozoan *Trypanosoma cruzi* (*T. cruzi*) [1–4]. Chagas disease is characterized by three phases: acute, indeterminate, and chronic. The heart is the most severely and frequently involved organ. A mild to severe acute myocarditis characterizes the cardiac involvement during the acute phase, with predominant mononuclear infiltrate around ruptured pseudocysts of parasites, and intense parasitism of myofibers that spontaneously subsides after 2–3 months in most cases. The indeterminate phase is a prolonged, clinically silent period – 10–30 years – that follows the acute phase. The patients present serological and/or parasitological evidence of infection with no symptoms or only minor disturbances of cardiac rhythm. The chronic phase evolves from the indeterminate phase in 10–30% of the cases in humans. Grossly, the heart is usually enlarged due to dilatation and hypertrophy, with 60–70% of patients presenting the characteristic apical aneurysm. Microscopically, a progressive, destructive and reparative chronic fibrosing myocarditis characterizes the chronic phase. Parasite antigens or, rarely, nests of *T. cruzi* are observed within cardiomyocytes and remain there as a result of host specific defense [1,3,5–7]. However, the mechanisms associated with the establishment/

* Corresponding author. Laboratory of Cellular and Molecular Cardiology, Department of Pathology, Faculty of Medicine of Ribeirão Preto, University of São Paulo, Av. Bandeirantes 3900, 14049-900 Ribeirão Preto, S.P., Brazil. Tel./fax: +55 16 3602 3130.
E-mail address: marossi@fmrp.usp.br (M.A. Rossi).

1286-4579/$ - see front matter © 2011 Institut Pasteur. Published by Elsevier Masson SAS. All rights reserved.
doi:10.1016/j.micinf.2011.08.010

maintenance of distinct clinical outcomes of Chagas disease appear to be complex and the transition to the chronic form remains to be elucidated.

Similar to CCC in humans, cardiac complications due to cardiomyopathy appear later in life in Duchenne muscular dystrophy and Becker muscular dystrophy, the most common X-linked recessive disorders resulting from mutations in the dystrophin gene that lead to an absence of or defect in the protein dystrophin in striated muscles. Dystrophin and associated glycoproteins form the so-called dystrophin glycoprotein complex, which contributes to cell shape, mechanical resistance, and contraction and force generation in cardiomyocytes [8]. It is known that mutations in the dystrophin gene result in membrane damage and necrosis that is associated with severe muscle degeneration and massive chronic inflammatory infiltrate [9]. Dystrophin reduction has been linked to end-stage cardiomyopathies and has been proposed as a common route to the induction of cardiomyopathy and heart failure [10,11]. Furthermore, dystrophin loss has been observed in different forms of acquired cardiomyopathies, such as post-viral myocarditis caused by Coxsackie virus B [12] and septic cardiomyopathy [13].

The development of cardiomyopathy in both Chagas disease and congenital dystrophinopathies occurs decades after infection or birth in humans, respectively. The present study tested the hypothesis that cardiac dystrophin levels are decreased during the early phase of the experimental infection by *T. cruzi* in mice and are maintained at low levels up to 100 days post infection (dpi); thus, explaining, in part, the late development of cardiomyopathy.

2. Materials and methods

2.1. Animals and experimental infection

The Brazil strain of *T. cruzi* was maintained in C3H mice (Jackson Laboratories, Bar Harbor, Maine, USA). Male CD1 mice (Charles River, Wilmington, MA, USA) were infected intraperitoneally at 10 weeks of age with 5×10^4 trypomastigotes. All mice were housed in the Institute for Animal Studies of the Albert Einstein College of Medicine and all protocols were approved by the Institutional Animal Care and Use Committee (Albert Einstein College of Medicine, New York) and by the Committee on Animal Research of the Faculty of Medicine of Ribeirão Preto (University of São Paulo, Brazil). The levels of parasitemia were evaluated using 5 μl of blood obtained from the tail vein of infected mice at days 15, 20, 30, 40, 60, 80 and 100 dpi. The mortality was evaluated throughout the experimental period.

2.2. Histopathological and morphometric analysis

Control and infected mice were sacrificed 30 and 100 dpi. These time points were chosen because 30 dpi is the peak of mortality associated with intense acute myocarditis with an inflammatory infiltrate mainly composed of lymphomononuclear cells and striking tissue parasitism and 100 dpi with cardiomegaly and mild to moderate chronic myocarditis characterized by infiltration of the interstitial space by mononuclear and spindle cells, interstitial fibrosis and the absence of tissue parasitism [14–16]. The hearts were rapidly removed, rinsed in ice-cold 0.9% NaCl solution and fixed in neutral 10% formalin for histological study or immediately frozen in liquid nitrogen-cooled isopentane for immunofluorescence study. Both ventricles from each heart were isolated and cut into two fragments by a mid-ventricular coronal section.

For histopathological study ($n = 6$/day/group), the samples were dehydrated, clarified, embedded in paraffin, stained with hematoxylin and eosin and picrosirius red and examined by light microscopy. The tissue sections stained with hematoxylin and eosin were used to evaluate the intensity of inflammation, the presence of amastigote nests and tissue damage. The slides stained with picrosirius red ($n = 6$/day/group) were used to evaluate fibrosis through collagen quantification.

For morphometric analysis ($n = 6$/day/group), the Leica QWin software (Leica Imaging Systems Ltd., Cambridge, England) in conjunction with a Leica microscope, videocamera, and an online computer was used. The number of inflammatory cells was determined by counting the number of mononuclear rounded interstitial cells (to exclude the spindle shaped fibroblastic cells) in the myocardium of the right and left ventricles in 10 microscope fields (40×1.6 magnification) per ventricle of each animal. To estimate the volume fraction (%) of fibrosis in picrosirius red-stained sections of the right and left ventricles, 10 microscope fields (400× magnifications) per ventricle of each animal were measured under polarized light with the QWin software. Measurements were made by a skilled observed blinded to the groups.

2.3. Immunofluorescence

For immunofluorescence microscopy, 5 μm frozen sections ($n = 6$/day/group) were transferred to silane-coated slides and fixed in cold acetone for 10 min. Immunolabeling was performed using primary antibody to dystrophin (rabbit polyclonal antibody anti-dystrophin, Santa Cruz Biotechnology Inc., Santa Cruz, CA, USA, dilution 1:200), diluted in 1% BSA and incubated overnight at 4 °C. Immunolabeling was performed using goat anti-rabbit fluorochrome-conjugated secondary antibody (FITC) (Vector Laboratories Inc., Burlingame, CA, USA) diluted 1:200 in HEPES 0.01 M and incubated for 1 h at room temperature. Omission of the primary antibodies served as negative control. Some sections were also labeled with phalloidin complexed to rhodamine (Alexa Fluor 594 phalloidin, Molecular Probes, Eugene, OR, USA) for visualization of actin. The nuclei were labeled with DAPI (Molecular Probes).

2.4. Western blotting

To determine the amount of dystrophin in control and chagasic hearts ($n = 5$/day/group), homogenates of the left and right ventricles were analyzed by immunoblotting at 30 and

100 dpi. Freshly excised hearts were washed in cold phosphate-buffered saline, the left and right ventricles were isolated and homogenized in extraction buffer with protease inhibition cocktail (Sigma–Aldrich, Saint Louis, MO, USA). Total heart protein (50 μg protein/well) was resolved on 5% SDS-PAGE and transferred to a nitrocellulose membrane (Hybond-ECL, Amersham Pharmacia Biotech, Amersham, UK). The membranes were blocked with 5% skimmed milk/TBS-T for 24 h and incubated overnight at 4 °C with primary antibody to dystrophin (rabbit polyclonal antibody anti-dystrophin, Santa Cruz Biotechnology Inc., dilution 1:500). The blots were washed and incubated with goat anti-rabbit HRP-conjugated secondary antibody (Santa Cruz Biotechnology Inc., diluted 1:20,000) for 1 h at room temperature. The membranes were washed, developed using ECL (Amersham Pharmacia Biotech), and exposed to Hyperfilm ECL (Amersham Pharmacia Biotech). GAPDH was used to normalize protein loading. The quantification was performed after scanning with a Kodak camera (Amersham Pharmacia Biotech) using Image J software (developed at the U.S. National Institute of Health and available on the Internet at http://rsb.info.nih.gov/nih-image). Values reported are optical densities expressed as arbitrary units (AU).

2.5. Cardiac gated magnetic resonance imaging (MRI)

The mice were imaged 15, 30, 60, and 100 dpi under inhalation anesthesia (1–2% isoflurane in 95% oxygen and 5% carbon dioxide) (n = 5/day/group). A set of standard, shielded, nonmagnetic electrocardiographic leads ending in silver wires were attached to the four limbs. The electrocardiographic signal was fed to a Gould Electrocardiograph amplifier associated with the Ponemah Physiology data acquisition system for monitoring the electrocardiogram; the R wave triggered a 5-V signal to gate the spectrometer. Images were acquired with a GE/Omega 9.4 T vertical wide-bore spectrometer operating at a ^{1}H frequency of 400 MHz and equipped with 50-mm shielded gradients (General Electric, Fremont, CA, USA) and a 40-mm ^{1}H imaging coil (RF Sensors, New York, NY, USA). Temperature within the coils was maintained at 30 °C using a water-cooling unit (Neslab Instrument, Inc., Portsmouth, NH, USA). This temperature prevented hypothermia in the anesthetized mice. After attachment of the cardiac gating leads, the mice were wrapped in a Teflon sheet and multi-slice spin echo imaging was performed to obtain short axis images of the heart. The gating delay was adjusted to collect data in systole or diastole. The following parameters were used to obtain 8 short axis slices: echo time, 18 ms; field of view, 51.2 mm; number of averages, 4; slice thickness, 1 mm; repetition time, approximately 0.2 s; matrix size, 128 × 256 (interpolated to 256 × 256). Several sets of 8 slices were acquired to define the entire heart and to obtain images in diastole and systole taking approximately 20–30 min per mouse. Data were transferred to a computer and analyzed using MATLAB-based software. Left ventricle and right ventricle dimensions in millimeters were determined from the images representing end-diastole. The left ventricular wall is the average of the anterior, posterior, lateral, and septal walls. The right ventricular internal dimension is the widest point of the right ventricular cavity.

2.6. Echocardiography

The mice were imaged 15, 30, 60, and 100 dpi (n = 5/day/group). They were lightly anesthetized with 1–2% isoflurane in 95% oxygen and 5% carbon dioxide; the chest wall was shaved and a small gel standoff was placed between the chest and a 30-MHz RMV-707 B scanhead interfaced with a Vevo 770 High-Resolution Imaging System (VisualSonics, Toronto, ON, Canada). High-resolution EKV Mode and B Mode images were acquired. Continuous, standard electrocardiogram was recorded using electrodes placed on the animal's extremities. Diastolic measurements were performed at the point of greatest cavity dimension, and systolic measurements were made at the point of minimal cavity dimension, using the leading edge method of the American Society of Echocardiography [17]. Ejection fraction was calculated and used as a determinant of left ventricular cardiac function.

2.7. Statistical analysis

Data were analyzed using GraphPad Prism 5 statistical program (GraphPad Software Inc., San Diego, CA, USA). Multiple comparisons were made using ANOVA followed by Bonferroni post-test. Comparisons between two groups were made using Student's t-test. The survival rate was expressed as the percentage of live animals. All data are expressed as mean ± SD. A level of significance of 5% was chosen to denote significant differences between mean values.

3. Results

3.1. Parasitemia and mortality

The mortality rate was 60% at 30 dpi with the remaining 40% of the infected mice surviving up to 100 dpi (Fig. 1A). Mice had a peak of parasitemia of 90 × 10^4 trypomastigotes/mL of plasma at day 20 dpi (Fig. 1B).

3.2. Histopathological analysis

Histological analysis demonstrated that control mice displayed normal cardiac fibers with regular interstitial space in the right (Fig. 2A) and left (Fig. 2B) ventricles. At 30 dpi there was an intense and diffuse myocarditis characterized by lymphomononuclear interstitial infiltrate, disruption of myofibers, multiple pseudocysts of amastigotes and enlargement of the interstitial space. Most of the infected myocytes were surrounded by this infiltrate. There was also perivascular inflammatory infiltrate (Fig. 2C, D). These findings were more evident in the right ventricle (Fig. 2C). At 60 dpi, the tissue parasitism decreased and the parasite pseudocysts were rare in both ventricles (data not shown). By 100 dpi, the number of lymphomononuclear inflammatory cells was reduced and no

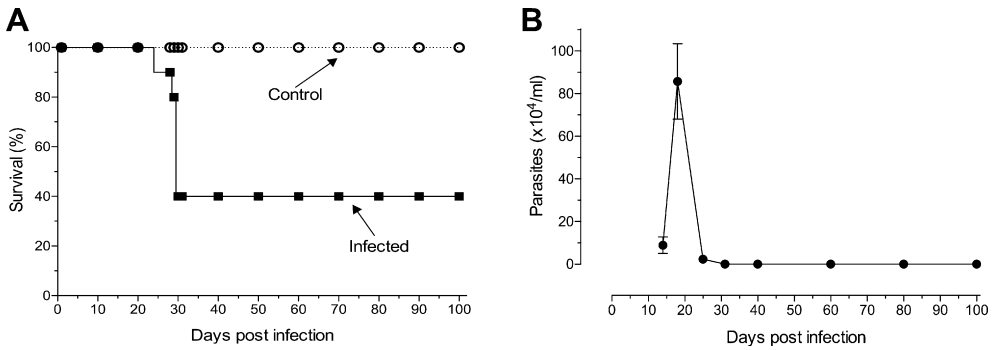

Fig. 1. Survival curve and parasitemia of control and CD1 mice infected with 5×10^4 trypomastigotes forms of *T. cruzi*. (A) Survival curve. The mortality rate peaked at 60% 30 dpi, 40% of the infected mice surviving to 100 dpi. (B) Parasitemia. Mice had a peak of parasitemia of 90×10^4 trypomastigotes/mL of plasma at day 20 pi. The results are representative of three different experiments, $n = 30$ animals.

parasites were detected (Fig. 2E, F). The number of interstitial mononuclear cells was quantified and was more pronounced at 30 dpi when compared to 100 dpi, especially in the right ventricle. The number of cells per field in the right ventricle increased 10 times by 30 dpi and dropped to 2.3 times at 100 dpi when compared to control (Fig. 2G). In the left ventricle, the increase in the number of cells per field at 30 dpi was increased by 4 times and dropped to 1.7 times at 100 dpi in comparison with values of controls (Fig. 2H).

The analysis of picrosirius red-stained sections under polarized light revealed mild myocardial fibrosis manifested by an increased amount of pericellular collagen (endomysial matrix) and mild perivascular fibrosis. These findings were more evident in the right ventricle (Fig. 3). The increase in the volume fraction of fibrosis in the right ventricle at 30 dpi was not statistically significant; however, at 100 dpi the increase was 600% (Fig. 3 upper left graph). In the left ventricle, the increase in the volume fraction of fibrosis at 30 dpi was also not significant but by 100 dpi the increase was 62% (Fig. 3 upper right graph).

3.3. Dystrophin analysis

Densitometric analysis of western blotting showed a significant reduction of dystrophin from 30 dpi up to 100 dpi. The immunofluorescence study revealed that dystrophin was focally reduced or completely lost in cardiomyocytes of infected mouse hearts. In order to determine whether the reduction in dystrophin expression was a consequence of myocytolytic necrosis, the sections were double-immunolabeled with antibody directed against dystrophin and with phalloidin complexed to rhodamine to detect actin in the cytoskeleton of the cardiomyocytes. At 30 dpi, as can be clearly seen in Fig. 4E, there are foci of myocytolysis or myocytolytic necrosis, as revealed by collapsed and clumped actin associated with loss of the dystrophin fluorescent signal, associated with infiltration by a great number of interstitial cells (Fig. 4F). Additionally, foci of cardiomyocytes showing undamaged actin or very mild actin lysis was observed with markedly reduced/loss of dystrophin fluorescent signal. At 100 dpi the foci of loss/reduction of dystrophin fluorescent signal was associated with undamaged actin or very mild actin lysis, without collapse of actin in cardiomyocytes, (Fig. 4H) and a small number of interstitial cells (Fig. 4I). There was uniform dystrophin staining in the myocardium obtained from uninfected age-matched mice (Fig. 4A–C).

3.4. Cardiac MRI

There was no significant difference in the left ventricular internal diameter in infected mice compared with uninfected controls during the period studied. However, the inner dimension of the right ventricle was significantly dilated from 30 to 100 dpi. This increase in right ventricle chamber dimension was 95% at 30 dpi, 80% at 60 dpi and 54% at 100 dpi in comparison with respective controls. There was no difference in the left ventricle wall thickness from 15 to 60 dpi. However, at 100 dpi, the increase was 11.4% in comparison with controls (Fig. 5).

3.5. Echocardiography

Infected mice did not show any change in the ejection fraction at 15 dpi in comparison with controls. However, there was a 23% reduction in the left ventricular ejection fraction at 30 dpi, 20% at 60 dpi and 20% at 100 dpi in comparison with respective controls (Fig. 6). The heart rate for control mice was 582.7 ± 41.84 bpm and a reduction of 10% was observed at 30 dpi (529.4 ± 18.64, $p < 0.05$). There was no difference between control and infected mice at 100 dpi (547.7 ± 32.34) ($n = 5$/day/group).

4. Discussion

This study shows for the first time that CD1 mice experimentally infected with the Brazil strain of *T. cruzi* present focal loss or reduction of sarcolemmal dystrophin expression at 30 dpi that persists until 100 dpi. Concurrently, utilizing cardiac MRI and echocardiography, we demonstrated that *T. cruzi*-infected CD1 mice developed a dilated cardiomyopathy, characterized by right ventricular dilatation and reduction in left ventricular ejection fraction at both 30 and 100 dpi.

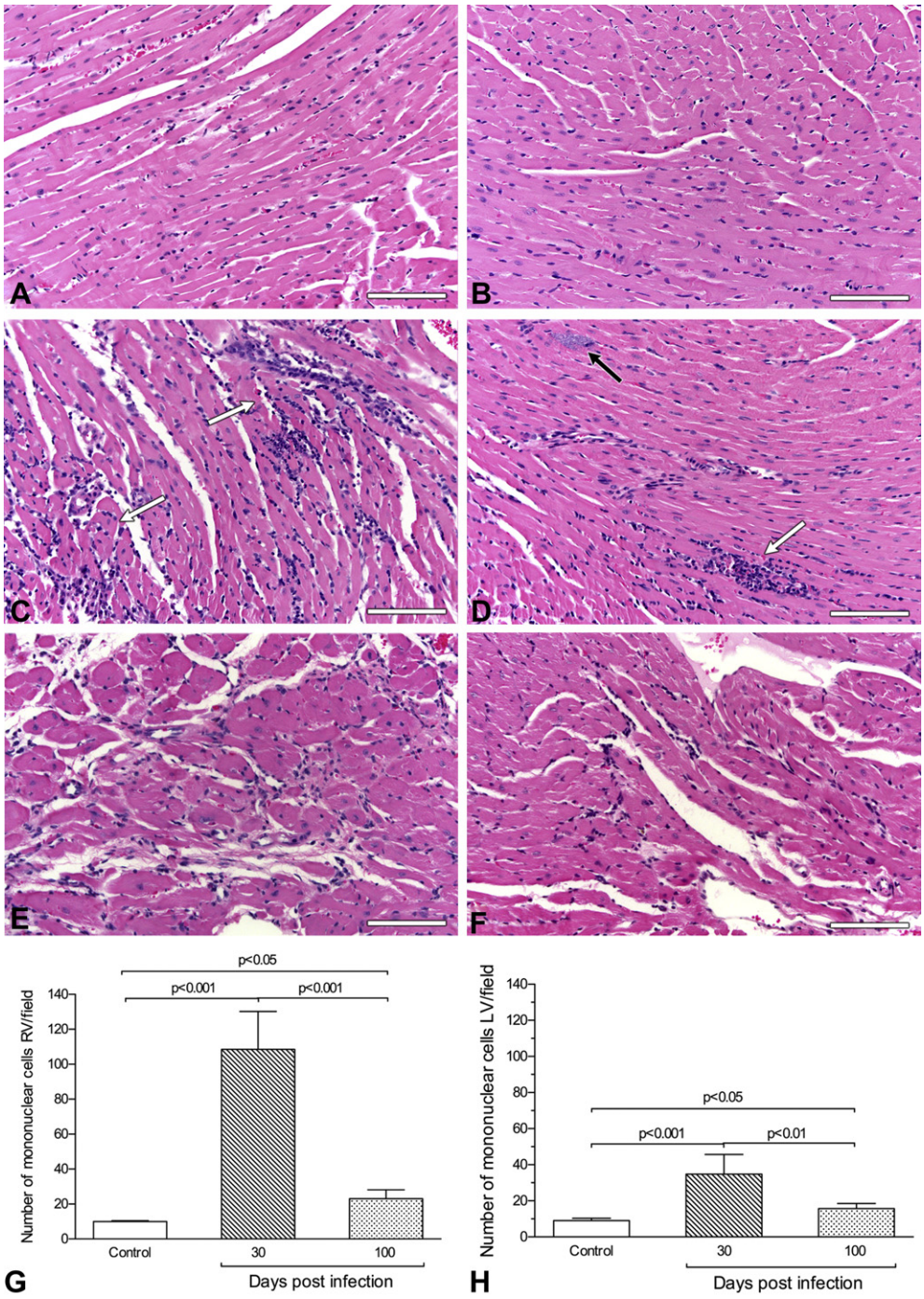

Fig. 2. Histological analysis demonstrated that control mice displayed normal cardiac fibers with regular interstitial space in the right (A) and left (B) ventricles. At 30 dpi there was an intense and diffuse myocarditis characterized by lymphomononuclear interstitial infiltrate (white arrow), multiple ruptured or unruptured pseudocysts (black arrow) and enlargement of the interstitial space (C and D). After 100 dpi, the number of lymphomononuclear inflammatory cells became significantly reduced and no parasites were detected (E and F). The numbers of interstitial mononuclear cells were quantified in both right and left ventricles. The number of cells was markedly increased at 30 dpi as compared to 100 dpi, mostly in the right ventricle (G and H). Bars = 100 μm, $n = 6$/day/group.

Cardiac complications in human chronic Chagas disease appear later in life, approximately 10–30 years after the initial infection. Chagas cardiomyopathy has also been described as a cardioneuropathy due to diminution in the number of parasympathetic ganglion cells in the heart [1,18], which occurs during the acute phase of the disease [19]. Köberle explained the late manifestations of Chagas disease, including Chagas heart disease, emphasizing that "*the denervation is the absolutely indispensable element for the appearance of these syndromes, but its development depends on the conjoint action of many other factors, among which the most important are (a) localization and intensity of denervation, (b) sensitivity of the affected organ to denervation and (c) solicitation and overloading of the damaged structure*" [1]. However, the factors

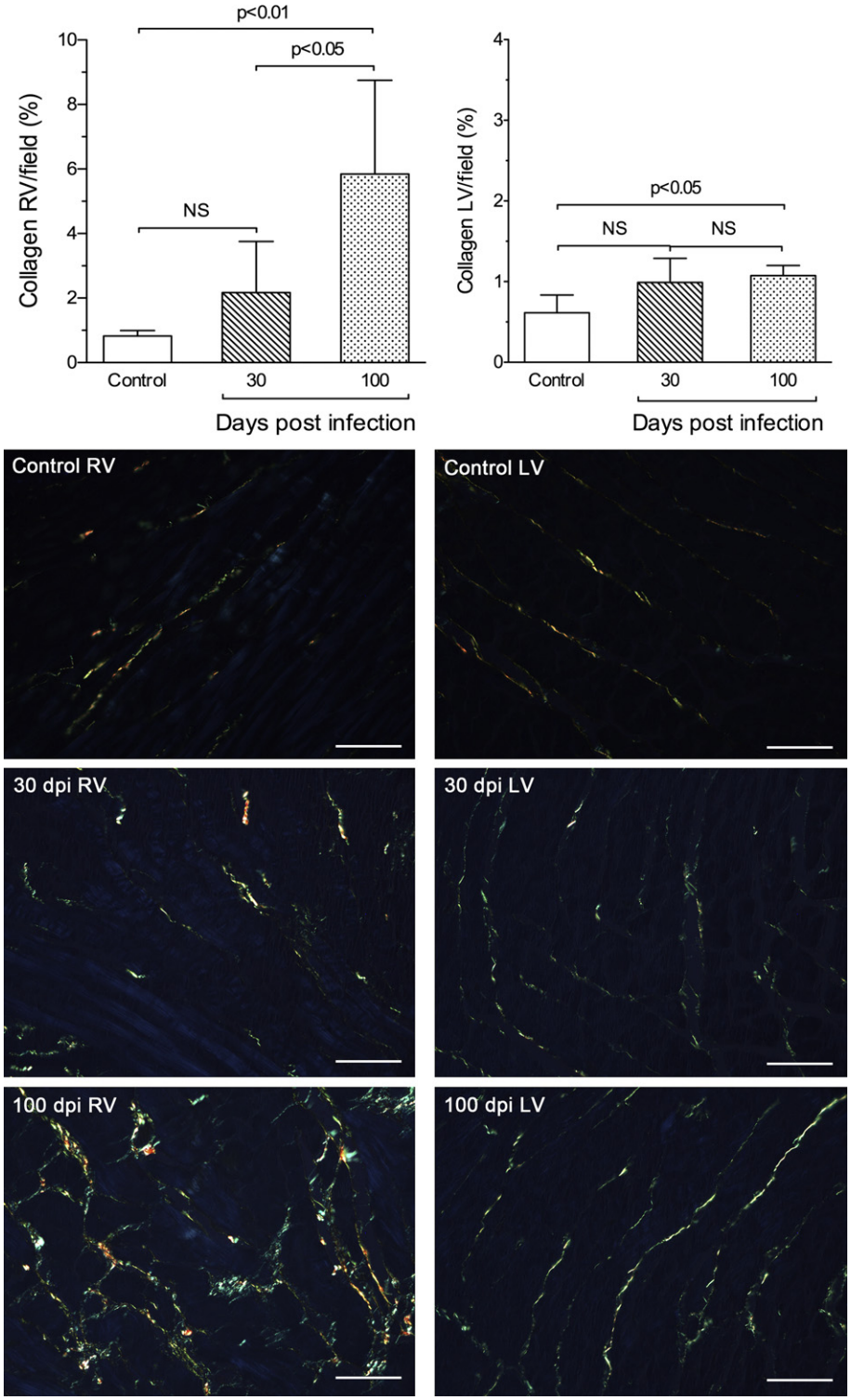

Fig. 3. Evaluation of interstitial collagen in picrosirius red-stained sections in control and *T. cruzi*-infected mice. The upper bar graphs show the mean fraction of fibrosis (%) in both right ventricle (RV, left graph) and left ventricle (LV, right graph). There was a tendency toward an increased amount of collagen at 30 dpi in both ventricles although the differences were not statistically significant. The mean amounts of collagen were significantly increased in the RV (600% higher) and LV (62% higher) at 100 dpi. Representative images illustrate these results clearly showing that the collagen increase was mainly perimysial. Bars = 50 μm, $n = 6$/day/group.

governing differential susceptibility to the late development of chronic Chagas cardiomyopathy are still unknown. The differential tissue tropism by different strains of *T. cruzi* was proposed to exert an important influence on the development of the late manifestations [20,21]. However, it is believed that the intensity of the pathophysiological alterations that occur at early stages of *T. cruzi* infection correlates positively with the severity of cardiomyopathy observed at the chronic phase of Chagas disease [1], regardless of the intrinsic mechanism or mechanisms.

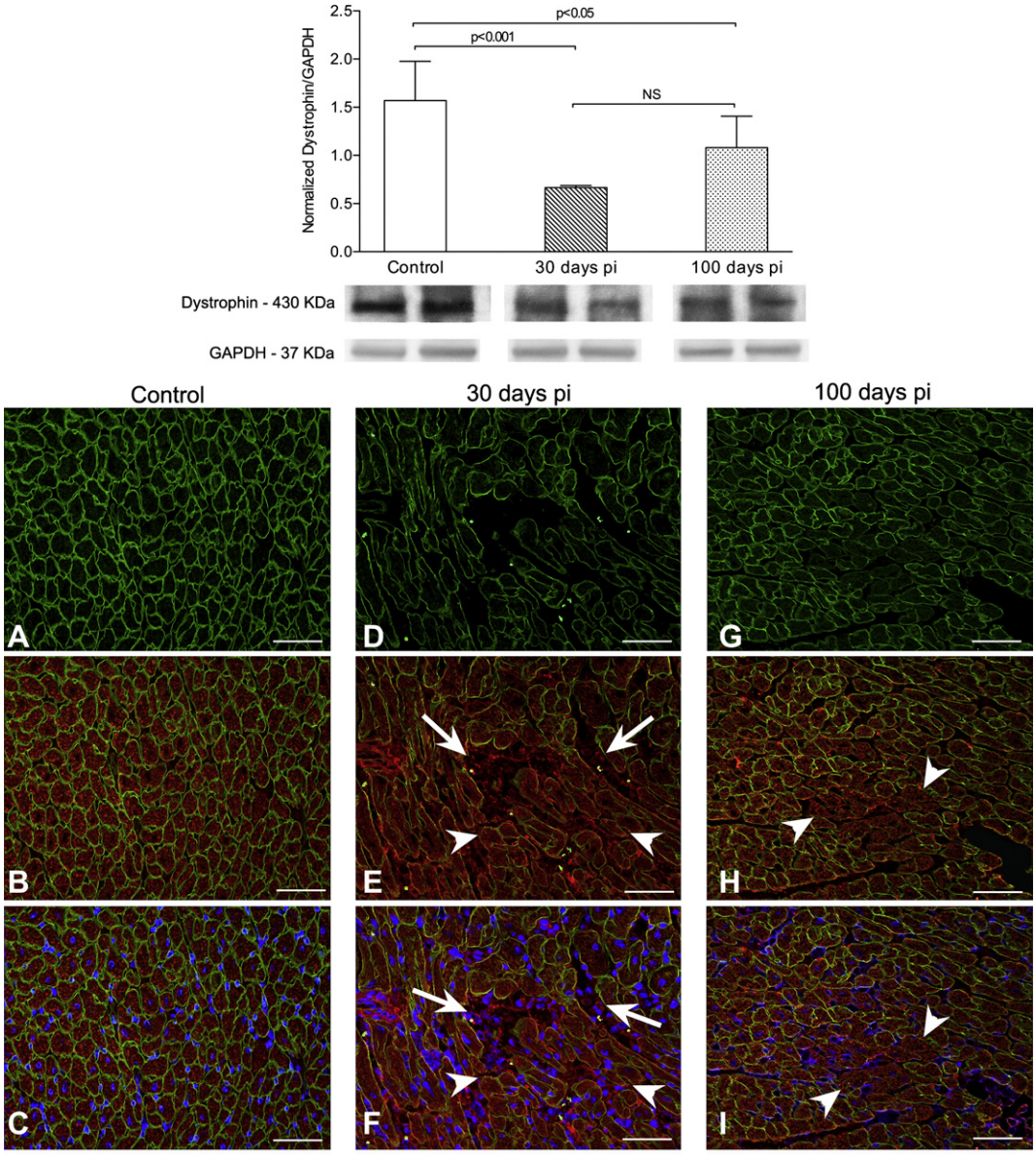

Fig. 4. Western blots and representative images of immunofluorescence for dystrophin in both control and *T. cruzi*-infected mice. Densitometric analysis of western blots (2 representative samples per group, $n = 6$/day/group) showed a significant reduction of dystrophin at 30 dpi sustained up to 100 dpi. GAPDH signal was used to normalize for loading differences between lanes. The immunofluorescence study revealed that dystrophin expression (green fluorescence) was focally reduced or completely lost at 30 dpi (D) and at 100 dpi (G) in cardiomyocytes of infected mouse hearts in comparison with controls. At 30 dpi, it can be clearly seen in E (merge of red fluorescent actin + green fluorescent dystrophin) that foci of collapsed and clumped actin are associated with dystrophin loss (white arrows). The merge of actin + dystrophin + DAPI (blue fluorescence) reveals a significant amount of interstitial cell infiltration in these foci (F, white arrows). At 100 dpi the foci of dystrophin loss/reduction was associated with undamaged actin or very mild actin lysis without collapse of actin in cardiomyocytes (H, white arrow heads) and was associated with a slightly increased number of interstitial cells (I, white arrow heads). Figures A, D and G show green fluorescence of dystrophin; Figures B, E and H show merge of dystrophin + red fluorescence of actin; Figures C, F and I show merge of dystrophin + actin + blue fluorescence of DAPI. Bars = 50 μm. (For interpretation of the references to color in this figure legend, the reader is referred to the web version of this article.)

As in *T. cruzi* infection, cardiac complications appear later in Duchenne (DMD) and Becker muscular dystrophies (BMD), the two most common and severe forms of dystrophinopathies. Although dystrophin gene mutations represent the primary cause of DMD and BMD, it has been demonstrated that the secondary processes, involving persistent inflammation with high levels of pro-inflammatory cytokines, likely sustain and exacerbate disease progression [22]. A recent study demonstrated that DMD patients with evidence of active myocarditis associated with myocyte damage and fibrosis had a faster progression to heart failure and death in comparison with DMD patients with evidence of healed myocarditis [23]. These observations indicate a special role for inflammation as an active participant in the disease process. It is, therefore, tempting to hypothesize that the occurrence of foci of myofibers with lost/reduced dystrophin levels and preserved actin filaments, as observed in the present study, suggests dystrophin loss/reduction as a possible role in

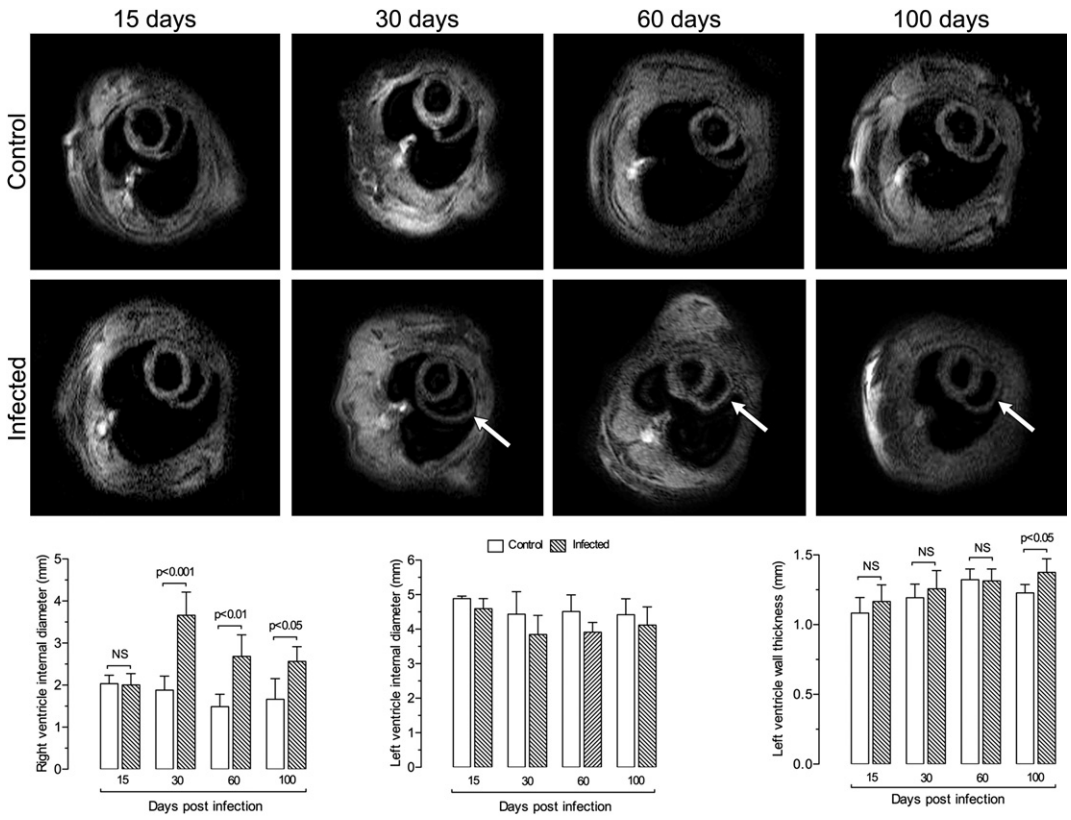

Fig. 5. Transverse magnetic resonance images of mice showing the short axis of the heart from 15 to 100 dpi and controls. The inner dimension of the right ventricle was significantly dilated from 30 to 100 dpi (white arrow); however, there was no difference in left ventricular internal diameter during the period studied. The left ventricle wall thickness was increased at 100 dpi. $n = 5$/day/group.

destabilizing the plasma membrane of cardiomyocytes in *T. cruzi*-induced cardiomyopathy. This could make the cardiomyocytes more susceptible to ancillary disease processes and consequent myofibrillar degeneration and lysis.

A shift from fatty acid to carbohydrate oxidation in the heart early after *T. cruzi* infection, prior to morphological and functional alterations, was previously observed [24]. It has been proposed that metabolic flexibility is lost early in the failing heart and can be considered a hallmark of maladaptation. This loss of metabolic flexibility starts, like hypertrophy, as an adaptive process that occurs before the onset of contractile dysfunction. In its advanced stages, loss of metabolic flexibility contributes to cardiac dysfunction leading to heart failure [25]. Metabolic perturbation in the heart has been shown to occur in different situations, such as in DMD patients [26], in progressive cardiac hypertrophy [27] and left ventricular dilatation [28], in acute myocardial infarction [29] and in the *mdx* mouse, an animal model with mutation in the dystrophin gene [25,30]. Results of studies that correlate cardiac metabolism and dystrophin-deficiency in hearts lead to the hypothesis that, beyond its purely mechanical role, dystrophin is critical for optimal cardiac metabolism-contraction coupling; dystrophin-deficiency thus causing a mismatch between energy supply and demand [30,31].

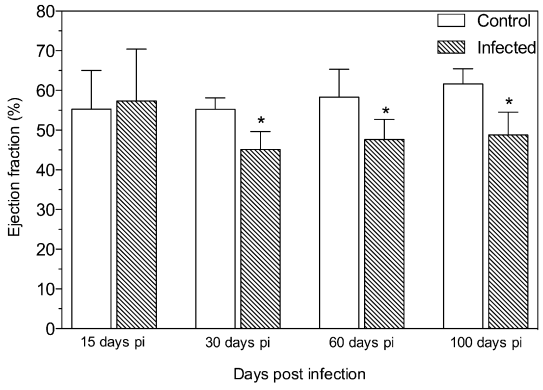

Fig. 6. Ejection fraction analysis. Infected mice did not show any change in the echocardiographic measurement at 15 dpi; however, they exhibited a significant reduction in LV ejection fraction at 30, 60 and 100 dpi. $n = 5$/day/group.

The findings in the present study allow us to discuss two possible mechanisms implicated in sarcolemmal dystrophin reduction in the hearts of mice experimentally infected with *T. cruzi*. First, myocardial ischemia is known to cause loss of sarcolemmal dystrophin and of other cytoskeleton proteins [13,32–34]. Microcirculatory abnormalities, resulting in hypoxia or ischemia, are considered to be involved in the genesis of acute and chronic myocarditis [2]. Aggregated platelets and occlusive thrombi in small epicardial and intramyocardial vessels [14] and histochemical evidence of hypoxic changes [35] have been described in the myocardium of mice chronically infected with *T. cruzi*. Numerous areas of focal vascular constriction, microaneurysm formation,

dilatation and proliferation of microvessels were seen early after infection with *T. cruzi* [36].

The vasculopathy in murine Chagas cardiomyopathy, which is accompanied by segmental vasospasm and dilatation and reduction in blood flow, is mediated in part by endothelin-1 [37] and could be ameliorated by verapamil, a drug that modulates vascular flow, endothelin synthesis/release, platelet aggregation and inflammation [38]. Furthermore, it was demonstrated that patients with chronic Chagas heart disease present an abnormal, endothelium-dependent, coronary vasodilating mechanism that may contribute to the genesis of the symptoms related to ischemic processes [39]. Such ischemic stress, induced by *T. cruzi* infection, could lead to the reduction of sarcolemmal dystrophin observed in mice at 30 dpi, a phenomenon that is maintained up to 100 dpi. Second, inflammatory mechanisms could also be involved in the dystrophin changes observed. Inflammation has been shown to play a key role in the activation of proteases responsible for dystrophin degradation [23,40]. Studies in a murine model demonstrated that cardiomyocytes infected with *T. cruzi* produce marked amounts of pro-inflammatory cytokines such as IFN-γ, IL-1β, TNF-α, IL-6 and TGFβ [41]. Pro-inflammatory cytokines have been demonstrated to exert their actions on target cells through nuclear factor-kappa B (NF-kB) [42,43], contributing to the dystrophic damage progression through activation of intracellular calcium-dependent proteases, mainly calpain, which can degrade cytoskeletal and membrane proteins, including dystrophin [44]. Recent work in our laboratory demonstrated that increased tissue expression of TNF-α, iNOS, NF-kB and calpain in the hearts of mice acutely infected with the Y strain of *T. cruzi* directly correlates with dystrophin loss (unpublished data).

The current investigation provides novel and mechanistic insight to clarify events that occur in the myocardium at 30 dpi and changes that are maintained up to 100 dpi, which might be related to the disease advancement. Based upon our findings we hypothesize that the loss/decreased levels of dystrophin in the acute phase of experimental *T. cruzi* infection, caused by ischemia and inflammation, contributes to the late development of a cardiomyopathy. This is a continuing interest of our laboratories.

Acknowledgments

The authors thank Lígia B. Santoro, Maria E. Riul, Mônica A. Abreu, Vicki L. Braunstein and Dazhi Zhao for excellent technical assistance. This study was supported by grants from the Fundação de Amparo à Pesquisa do Estado de São Paulo (FAPESP 07/58843-2; 07/59448-0; 09/17787-8; 09/53544-2; 09/54010-1; 10/19216-5; 10/18629-4; 10/13199-1), Conselho Nacional de Desenvolvimento Científico e Tecnológico (CNPq 472419/2009-9; 150723/2010-5), National Institutes of Health AI076248 (HBT). CMP and MRC were supported by a Fogarty International Training Grant D43-TW007129 (HBT).

References

[1] F. Köberle, Chagas' disease and Chagas' syndromes: the pathology of American trypanosomiasis, Adv. Parasitol. 6 (1968) 63–116.
[2] M.A. Rossi, Microvascular changes as a cause of chronic cardiomyopathy in Chagas' disease, Am. Heart J. 120 (1990) 233–236.
[3] M.A. Rossi, R.B. Bestetti, The challenge of chagasic cardiomyopathy. The pathologic roles of autonomic abnormalities, autoimmune mechanisms and microvascular changes, and therapeutic implications, Cardiology 86 (1995) 1–7.
[4] H.B. Tanowitz, F.S. Machado, L.A. Jelicks, J. Shirani, A.C. de Carvalho, D.C. Spray, S.M. Factor, L.V. Kirchhoff, L.M. Weiss, Perspectives on *Trypanosoma cruzi*-induced heart disease (Chagas disease), Prog. Cardiovasc. Dis. 51 (2009) 524–539.
[5] M.L. Higuchi, L.A. Benvenuti, M. Martins Reis, M. Metzger, Pathophysiology of the heart in Chagas' disease: current status and new developments, Cardiovasc. Res. 60 (2003) 96–107.
[6] M.A. Rossi, S.G. Ramos, R.B. Bestetti, Chagas' heart disease: clinical-pathological correlation, Front. Biosci. 8 (2003) e94–e109.
[7] M.A. Rossi, H.B. Tanowitz, L.M. Malvestio, M.R. Celes, E.C. Campos, V. Blefari, C.M. Prado, Coronary microvascular disease in chronic Chagas cardiomyopathy including an overview on history, pathology, and other proposed pathogenic mechanisms, PLoS Negl. Trop. Dis. 4 (2010) e674.
[8] M.J. Allikian, E.M. McNally, Processing and assembly of the dystrophin glycoprotein complex, Traffic 8 (2007) 177–183.
[9] A.E. Emery, The muscular dystrophies, Lancet 359 (2002) 687–695.
[10] A. Kumar, N. Khandelwal, R. Malya, M.B. Reid, A.M. Boriek, Loss of dystrophin causes aberrant mechanotransduction in skeletal muscle fibers, FASEB J. 18 (2004) 102–113.
[11] T. Kawada, F. Masui, A. Tezuka, T. Ebisawa, H. Kumagai, M. Nakazawa, T. Toyo-Oka, A novel scheme of dystrophin disruption for the progression of advanced heart failure, Biochim. Biophys. Acta 1751 (2005) 73–81.
[12] C. Badorff, G.H. Lee, B.J. Lamphear, M.E. Martone, K.P. Campbell, R. E. Rhoads, K.U. Knowlton, Enteroviral protease 2A cleaves dystrophin: evidence of cytoskeletal disruption in an acquired cardiomyopathy, Nat. Med. 5 (1999) 320–326.
[13] M.R. Celes, D. Torres-Dueñas, L.M. Malvestio, V. Blefari, E.C. Campos, S.G. Ramos, C.M. Prado, F.Q. Cunha, M.A. Rossi, Disruption of sarcolemmal dystrophin and beta-dystroglycan may be a potential mechanism for myocardial dysfunction in severe sepsis, Lab. Invest. 90 (2010) 531–542.
[14] M.A. Rossi, S. Gonçalves, R. Ribeiro-dos-Santos, Experimental *Trypanosoma cruzi* cardiomyopathy in BALB/c mice. The potential role of intravascular platelet aggregation in its genesis, Am. J. Pathol. 114 (1984) 209–216.
[15] L.A. Jelicks, J. Shirani, M. Wittner, M. Chandra, L.M. Weiss, S.M. Factor, I. Bekirov, V.L. Braunstein, L. Chan, H. Huang, H.B. Tanowitz, Application of cardiac gated magnetic resonance imaging in murine Chagas' disease, Am. J. Trop. Med. Hyg. 61 (1999) 207–214.
[16] H.B. Tanowitz, H. Huang, L.A. Jelicks, M. Chandra, M.L. Loredo, L.M. Weiss, S.M. Factor, V. Shtutin, S. Mukherjee, R.N. Kitsis, G.J. Christ, M. Wittner, J. Shirani, Y.Y. Kisanuki, M. Yanagisawa, Role of endothelin 1 in the pathogenesis of chronic chagasic heart disease, Infect. Immun. 73 (2005) 2496–2503.
[17] N.B. Schiller, P.M. Shah, M. Crawford, A. De Maria, R. Devereux, H. Feigenbaum, H. Gutgesell, N. Reichek, D. Sahn, I. Schnittger, et al., Recommendations for quantitation of the left ventricle by two-dimensional echocardiography. American Society of Echocardiography Committee on Standards, Subcommittee on Quantitation of Two-Dimensional Echocardiograms, J. Am. Soc. Echocardiogr 2 (1989) 358–367.
[18] F. Köberle, Die Chagaskrankleit – ihre Pathogenese und ihre Bedeutung als Volksseuche, Tropenmed. Parasitol. 10 (1959) 236–268.
[19] R.M. Arantes, H.H. Marche, M.T. Bahia, F.Q. Cunha, M.A. Rossi, J.S. Silva, Interferon-gamma-induced nitric oxide causes intrinsic intestinal denervation in *Trypanosoma cruzi*-infected mice, Am. J. Pathol. 164 (2004) 1361–1368.

[20] D.E. Bice, R. Zeledon, Comparison of infectivity of strains of *Trypanosoma cruzi* (Chagas, 1909), J. Parasitol. 56 (1970) 663–670.
[21] R.C. Melo, Z. Brener, Tissue tropism of different *Trypanosoma cruzi* strains, J. Parasitol. 64 (1978) 475–482.
[22] M.J. Spencer, J.G. Tidball, Do immune cells promote the pathology of dystrophin-deficient myopathies? Neuromuscul. Disord. 11 (2001) 556–564.
[23] S. Mavrogeni, A. Papavasiliou, K. Spargias, P. Constandoulakis, G. Papadopoulos, E. Karanasios, D. Georgakopoulos, G. Kolovou, E. Demerouti, S. Polymeros, L. Kaklamanis, A. Magoutas, E. Papadopoulou, V. Markussis, D.V. Cokkinos, Myocardial inflammation in Duchenne Muscular Dystrophy as a precipitating factor for heart failure: a prospective study, BMC Neurol. 10 (2010) 33–40.
[24] C.M. Prado, E.J. Fine, W. Koba, D. Zhao, M.A. Rossi, H.B. Tanowitz, L. A. Jelicks, Micro-positron emission tomography in the evaluation of *Trypanosoma cruzi*-induced heart disease: comparison with other modalities, Am. J. Trop. Med. Hyg. 81 (2009) 900–905.
[25] H. Taegtmeyer, L. Golfman, S. Sharma, P. Razeghi, M. van Arsdall, Linking gene expression to function: metabolic flexibility in the normal and diseased heart, Ann. N. Y. Acad. Sci. 1015 (2004) 202–213.
[26] J.K. Perloff, E. Henze, H.R. Schelbert, Alterations in regional myocardial metabolism, perfusion, and wall motion in Duchenne muscular dystrophy studied by radionuclide imaging, Circulation 69 (1984) 33–42.
[27] N. Handa, Y. Magata, T. Mukai, T. Nishina, J. Konishi, M. Komeda, Quantitative FDG-uptake by positron emission tomography in progressive hypertrophy of rat hearts in vivo, Ann. Nucl. Med. 21 (2007) 569–576.
[28] L. Stegger, K.P. Schäfers, U. Flögel, L. Livieratos, S. Hermann, C. Jacoby, P. Keul, E.M. Conway, O. Schober, J. Schrader, B. Levkau, M. Schäfers, Monitoring left ventricular dilation in mice with PET, J. Nucl. Med. 46 (2005) 1516–1521.
[29] C. Godino, C. Messa, L. Gianolli, C. Landoni, A. Margonato, M. Cera, C. Stefano, D. Cianflone, F. Fazio, A. Maseri, Multifocal, persistent cardiac uptake of [18-f]-fluoro-deoxy-glucose detected by positron emission tomography in patients with acute myocardial infarction, Circ. J. 72 (2008) 1821–1828.
[30] W. Zhang, M. ten Hove, J.E. Schneider, D.J. Stuckey, L. Sebag-Montefiore, B.L. Bia, G.K. Radda, K.E. Davies, S. Neubauer, K. Clarke, Abnormal cardiac morphology, function and energy metabolism in the dystrophic mdx mouse: an MRI and MRS study, J. Mol. Cell. Cardiol. 45 (2008) 754–760.
[31] M. Khairallah, R. Khairallah, M.E. Young, J.R. Dyck, B.J. Petrof, C. Des Rosiers, Metabolic and signaling alterations in dystrophin-deficient hearts precede overt cardiomyopathy, J. Mol. Cell. Cardiol. 43 (2007) 119–129.
[32] M. Rodríguez, W.J. Cai, S. Kostin, B.R. Lucchesi, J. Schaper, Ischemia depletes dystrophin and inhibits protein synthesis in the canine heart: mechanisms of myocardial ischemic injury, J. Mol. Cell. Cardiol. 38 (2005) 723–733.
[33] E.C. Campos, M.M. Romano, C.M. Prado, M.A. Rossi, Isoproterenol induces primary loss of dystrophin in rat hearts: correlation with myocardial injury, Int. J. Exp. Pathol. 89 (2008) 367–381.
[34] S.C. Amstrong, C.A. Latham, C.L. Shivell, C.E. Ganote, Ischemic loss of sarcolemmal dystrophin and spectrin: correlation with myocardial injury, J. Mol. Cell. Cardiol. 33 (2001) 1165–1179.
[35] M.A. Rossi, S.G. Carobrez, Experimental *Trypanosoma cruzi* cardiomyopathy in BALB/c mice: histochemical evidence of hypoxic changes in the myocardium, Br. J. Exp. Pathol. 66 (1985) 155–160.
[36] S.M. Factor, S. Cho, M. Wittner, H. Tanowitz, Abnormalities of the coronary microcirculation in acute murine Chagas' disease, Am. J. Trop. Med. Hyg. 34 (1985) 246–253.
[37] H.B. Tanowitz, D.K. Kaul, B. Chen, S.A. Morris, S.M. Factor, L.M. Weiss, M. Wittner, Compromised microcirculation in acute murine *Trypanosoma cruzi* infection, J. Parasitol. 82 (1996) 124–130.
[38] A.P. De Souza, H.B. Tanowitz, M. Chandra, V. Shtutin, L.M. Weiss, S.A. Morris, S.M. Factor, H. Huang, M. Wittner, J. Shirani, L.A. Jelicks, Effects of early and late verapamil administration on the development of cardiomyopathy in experimental chronic *Trypanosoma cruzi* (Brazil strain) infection, Parasitol. Res. 92 (2004) 496–501.
[39] F.W. Torres, H. Acquatella, J.A. Condado, R. Dinsmore, I.F. Palacios, Coronary vascular reactivity is abnormal in patients with Chagas' heart disease, Am. Heart J. 129 (1995) 995–1001.
[40] K. Nozaki, A. Das, S.K. Ray, N.L. Banik, Calpain inhibition attenuates intracellular changes in muscle cells in response to extracellular inflammatory stimulation, Exp. Neurol. 225 (2010) 430–435.
[41] M.M. Teixeira, R.T. Gazzinelli, J.S. Silva, Chemokines, inflammation and *Trypanosoma cruzi* infection, Trends Parasitol. 18 (2002) 262–265.
[42] A. Kumar, A.M. Boriek, Mechanical stress activates the nuclear factor-kappaB pathway in skeletal muscle fibers: a possible role in Duchenne muscular dystrophy, FASEB J. 17 (2003) 386–396.
[43] J.G. Tidball, Inflammatory processes in muscle injury and repair, Am. J. Physiol. Regul. Integr. Comp. Physiol. 288 (2005) R345–R353.
[44] S.I. Zaidi, H.T. Narahara, Degradation of skeletal muscle plasma membrane proteins by calpain, J. Membr. Biol. 110 (1989) 209–216.